Carbohydrate Polymers 100 (2014) 55–64

Contents lists available at ScienceDirect

Carbohydrate Polymers

journal homepage: www.elsevier.com/locate/carbpol

Novel cellulose based materials for safe and efficient wound treatment

Zdenka Peršin[a,e], Uroš Maver[a,b,c], Tanja Pivec[d,e], Tina Maver[e], Alenka Vesel[a], Miran Mozetič[f], Karin Stana-Kleinschek[a,e,*]

[a] Center of Excellence Polymer Materials and Technologies, Slovenia
[b] National Institute of Chemistry, Ljubljana, Slovenia
[c] Faculty of Medicine, University of Maribor, Slovenia
[d] Predilnica Litija d.o.o., Slovenia
[e] Faculty of Mechanical Engineering, University of Maribor, Slovenia
[f] Jožef Stefan Institute, Ljubljana, Slovenia

ARTICLE INFO

Article history:
Received 3 September 2012
Received in revised form 27 February 2013
Accepted 25 March 2013
Available online 23 April 2013

Keywords:
Hydrophilicity
Antimicrobial activity
Plasma treatment
Wound dressing materials

ABSTRACT

The present study aims at achieving effects of improved hydrophilicity and microorganism inhibition, which are rarely simultaneously present in wound dressings. Viscose fibers in their non-woven form were modified using two different pathways. Effects of a two-step procedure, i.e. alkaline or oxygen plasma treatment followed by the attachment of silver chloride nanoparticles were compared to a one-step procedure, i.e. ammonium plasma treatment, which results in both desired material characteristics simultaneously.

The surface properties of untreated and differently modified cellulose samples were analyzed by X-ray photoelectron spectroscopy (XPS), scanning electron microscopy (SEM), in vitro silver release, and hydrophilicity measurements. The treatment effect on antimicrobial activity was determined by the AATCC 100-1999 standard test. In light of the introduced wound dressing preparation procedures and the desired wound dressing characteristics, the effectiveness of the used procedures was evaluated. Antimicrobial activity was proven against all Gram negative bacteria, while the Gram positive bacteria survive the as-prepared samples. Hydrophilicity was proven to be excellent using both preparation procedures. The mentioned results prove the potential of the used procedures and encourage future developments toward the clinical proof of concept.

1. Introduction

Successful wound treatment is not possible without assuring and maintaining proper hydrophilicity and an effective antimicrobial activity (Thomas, 2008). There are many known super-hydrophilic materials of synthetic origin (Chen & Chiang, 2010; Klode et al., 2011; Lalani & Liu, 2012), which can be used in wound treatment. Although their hydrophilic properties are excellent, they have several other drawbacks, ranging from their inability to be additionally functionalized to gain antimicrobial properties, their possible irritation on human skin and a higher production cost (Klode et al., 2011). Natural cellulose like cotton is rarely used as a wound dressing absorber due to rather low purity as well as relatively high production costs. Cellulosic fibers, i.e. viscose, in a form of woven or non-woven textiles are the most used wound dressing base materials. Although the sorption capacity as well as the wettability rate of viscose is much better than for many other similar materials (e.g. lyocell, modal), these properties are still not optimal and definitely below the capacities of alginate (Rowe, Sheskey, & Quinn, 2009).

Materials with a superior sorption capability combined with an efficient infection control, with minimized unwanted side effects are nowadays sought for the preparation of advanced, healing promoting wound dressings. In order to achieve both desired effects, several procedures are available that mostly combine different functionalization steps one after another. Improvement of cellulose absorption properties is mostly acquired by co-polimerisation (Hengstberger, Kaltenecker, & Oppermann, 1999), doping (Junping, Xin, Dequan, & Li, 2010), deposition (Hyde et al., 2011) and by chemical processes, e.g. alkaline treatment, bleaching (Durso, 1978; Fengel & Wegener, 1984; Freytag & Donzé, 1983; Lewin, 1984). Controlling bacterial or fungal growth on fabric can be achieved using biologically-active polymers (Breitwieser, Spirk, et al., in press; Chekmareva, 2002), by the inclusion of potential antimicrobial compounds, e.g. collagen (Hart, Silcock, & Gunnigle, 2002),

* Corresponding author at: University of Maribor, Faculty of Mechanical Engineering, Institute for Engineering Materials and Design, Smetanova 17, SI-2000 Maribor, Slovenia. Tel.: +386 2 220 7881; fax: +386 2 220 7990.
E-mail addresses: karin.stana@um.si, karin.stana@uni-mb.si (K. Stana-Kleinschek).

0144-8617/$ – see front matter © 2013 Elsevier Ltd. All rights reserved.
http://dx.doi.org/10.1016/j.carbpol.2013.03.082

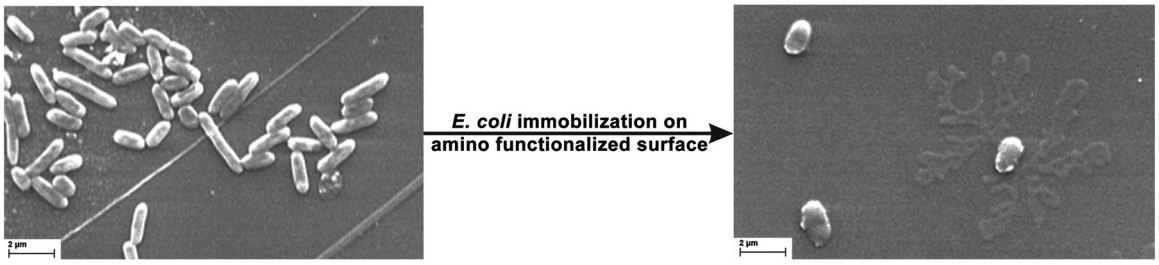

Fig. 1. Interaction of bacterial cells with surfaces with amino functional groups leads to their destruction (Reichel, 2012).

and chitosan (Baohua, Hu, & Meng, 2009; Jing, Zhang, Zhang, Zhao, & Yuan, 2009; Madhumathi et al., 2010; Watthanaphanit, Supaphol, Tamura, Tokura, & Rujiravanit, 2010; Wu et al., 2004), by binding drugs onto the polymer surface (Kontogiannopoulos, Assimopoulou, Tsivintzelis, Panayiotou, & Papageorgiou, 2011; Watanakunakorn & Glotzbecker, 1978) or by chemically modifying the polymer structure through introduction of various functional groups such as amino (Gilbert & Moore, 2005; Mikhaylova et al., 2011; Zemljic Fras, Persin, & Stenius, 2009), hydroxyl, carboxyl, aldehyde (Chekmareva, 2002; Hart, Silcock, & Gunnigle, 2002), and combinations of carboxyl and amino, epoxy, methoxy, thiol and sulphone. Amino groups are known to adsorb onto the bacterial cell wall, which provides the molecules bearing this functional groups to diffuse into the cell interior, where the disruption of the cytoplasmic membrane finally leads to the bacterial cell destruction (Reichel, 2012). Typical bacterial cell destruction due to the interaction with an amino functionalized surface is shown in Fig. 1.

Many heavy metal cations (i.e. Hg^{2+}, Pb^{2+}) have antimicrobial activity, but are very toxic. Other metal ions such as e.g. cooper (Cady, Behnke, & Strickland, 2011; Esteban-Cubillo, Pecharromán, Aguilar, & Moya, 2006), and zinc (Lee & Huang, 1995) have been identified as acting destructively toward microbes, but were not found safe for patients, unless prepared in specific forms (Fraser, Cuttle, Kempf, & Kimble, 2004; Percival, Bowler, & Russell, 2005) and the environment.

Many different products with high antimicrobial activities are commercially available for quite a long time (Kuroyanagi et al., 1994; Robb & Nathan, 1981). Among these, is silver certainly one of the most important antimicrobial agents used in wound treatment (Corum et al., 2011). Silvers broad-spectrum antimicrobial activity is still not fully understood, but is believed to be connected with the silvers ability to interact and denaturize various biological macromolecules by interacting with their thiol-, carboxyl, phosphate-, and imidazole-functional groups (the so-called oligodynamic effect). For example, these interactions are the cause of interferences in the respiratory chain in the cytochromes of some bacteria; additionally can silver ions interfere with components of the microbial electron transport system, bind DNA, and inhibit DNA replication (Lansdown, 2002; Lok et al., 2006). While both mentioned cases encourage further use of silver based products, is the lack of specificity of such interactions also the reason for citocompatibility issues (Eid & Azzazy, 2012; Kokura et al., 2010; Liu, Sonshine, Shervani, & Hurt, 2010; Seetharaman et al., 2011). In recent years several different research groups pointed out that the silver release from wound dressings can have cytotoxic effects on the healthy tissue (AshaRani, Low Kah Mun, Hande, & Valiyaveettil, 2008; Kim, Yang, & Ryu, 2010; Lina et al., 2010). Due to this, novel approaches were developed, which can either lead to a safe silver binding, meaning that the antimicrobial activity is preserved, while the silver stays bound to the wound dressing over the course of its application (Breitwieser, Moghaddam, et al., in press; Eid & Azzazy, 2012) or rely on the use of new antimicrobial agents that act specifically only on desired pathogens (Infante et al., 2004; Malmsten, 2011).

In this study we prepared two different procedures to maximize the efficacy of achievement desired wound dressing characteristics. The developed procedures were used for the preparation of cellulose-based wound dressing materials and were compared regarding the desired dressing surface characteristics—optimal hydrophilicity and a safe, efficient antimicrobial activity. The two-step procedure consists of a pre-treatment, i.e. alkaline or oxygen plasma treatment for improving absorption properties, which is followed by a sol–gel procedure for the attachment of antimicrobial silver chloride nanoparticles. The applied sol–gel method was chosen due to its capability to effectively attach silver chloride nanoparticles onto cellulose materials, as shown in our previous study (Pivec et al., 2012). A similar formulation was also used by other researchers (Tomsic et al., 2009) with the same emphasis–improvement of the potential to be used in the development of future wound dressings. The second used pathway was a one-step procedure, introducing plasma treatment using ammonium gas to simultaneously obtain improved sorption and antimicrobial properties.

Elemental surface chemical composition was obtained by X-ray photoelectron spectroscopy, while the sample morphology was investigated using scanning electron microscopy (SEM). Silver release from materials was monitored using the Franz static diffusion cell, while its concentration was determined using atomic absorbance spectrometry (AAS). Improved viscose non-woven hydrophilic properties were characterized by water up take monitoring, while antimicrobial properties were determined by AATCC 100-1999 standard test (American Association of Textile and Colorists, 1999).

2. Experimental

2.1. Materials

A cellulose material, as regenerated cellulose fibers (CV) in its non-woven form was used, as produced by KEMEX, The Netherlands. The surface mass of the fabrics was 175 g/m^2 (SIST ISO 3801) and the thickness under normal conditions was about 1.7 mm (SIST EN ISO 5084). The untreated sample is noted as U.

2.2. Preparation procedures

2.2.1. Two-step pathway

1.STEP-a: Alkaline treatment

Viscose non-woven was impregnated using an alkaline solution (53 g/L of NaOH; ratio 1:10; pH = 13.1). The treatment was performed for 5 min at room temperature.

After treatment, the samples were rinsed with distilled water until the conductivity of the rinsing water reached a conductivity of 3 μS/cm. The samples in a stretch form were dried in an oven

(Werner Mathis Ag, Switzerland) at 70 °C. The sample, treated only by NaOH is noted as A.

1 STEP-b: Oxygen plasma treatment

Air-conditioned (20 °C and 65% RH for 24 h) reference viscose sample (CV), was exposed to non-equilibrium plasma created in oxygen gas. The discharge chamber was a glass cylinder with the length of 30 cm and the inner diameter of 27 cm terminated by side plates made from aluminum. Plasma was excited by a radiofrequency (RF) generator operating at the standard industrial frequency of 27.12 MHz and the nominal power of 5 kW. The output power was fixed to about 500 W, creating almost perfectly uniform plasma in the entire discharge chamber. The plasma system was connected with vacuum system pumped with a two-stage oil rotary pump with a pumping speed of 40 m^3/h. During the experiment, the pressure was fixed at 75 Pa. The samples (22 cm × 22 cm) were exposed for 10 min to commercially available oxygen that was leaked into discharge chamber. Oxygen plasma treated sample is noted as OP.

2 STEP: Attachment of silver chloride nanoparticles

To attach silver chloride nanoparticles, a combination of iSys Ag with a silver concentration of 8.4 mg/g (CHT, Germany) as the source for the particles and iSys LTX (CHT, Germany) as the inorganic–organic binder, were used. Kollasol CDO (CHT, Germany) was used as a wetting agent. The preparation was performed as follows: firstly water solutions of all the mentioned precursors were prepared—iSys LTX (5 g/L), iSys Ag (5 g/L) and Kollasol (0.7 g/L). Samples of the proposed wound dressing material (in the form of viscose non-woven) were impregnated in a solution with the bath ratio 1:30 at room temperature for 1 h (amount of dissolved silver was therefore 1.26 mg). After the impregnation step, all samples were wrung-out with a foulard (Werner Mathis Ag, Switzerland) at a pressure of 4 bar between cylinders and their speed of rotation at 0.5 m/min. The final treatment of the samples involved oven drying in a stretched state at 80 °C, and condensation for 1 min at 150 °C (Werner Mathis Ag, Switzerland). The sample treated by both steps of the two-step pathway procedure is noted as either AS (for the alkaline treatment, followed by the attachment of silver chloride nanoparticles) or as OPS (for the oxygen plasma treatment, followed by the attachment of the silver chloride nanoparticles).

2.2.2. One-step pathway

2.2.2.1. Ammonium plasma treatment. Air-conditioned (20 °C and 65% RH for 24 h) reference viscose sample (CV), was exposed to non-equilibrium plasma created in ammonia gas. The reactor, made from borosilicate glass, was a 60 cm long cylindrical tube, with inner diameter of 3.6 cm. A water-cooled copper tube of diameter 4 mm and 5 turns was wounded onto the plasma reactor and connected to a radiofrequency (RF) generator via a matching network. The RF generator operated at the standard industrial frequency of 13.56 MHz and an adjustable power up to 1200 W. The cylindrical tube reactor was connected to the gas inlet system on one side, while on the other side it was pumped continuously with a two stage rotary vane vacuum pump with the ultimate pressure well below 1 Pa and a nominal pumping speed of 0.022 $m^3\ s^{-1}$ constant in a range of pressures from 1 to 104 Pa. NH_3 gas was leaked into the system through a manually controlled leak valve allowing establishment of the optimum pressure, of about 150 Pa, inside the plasma reactor, regarding homogeneity of plasma luminosity. The samples were cut to pieces of 3 cm × 12 cm and treated with ammonia gas for 300 s. The sample prepared by the one-step pathway procedure is noted as NP.

Plasma parameters for both plasma treatment procedures were determined using a double Langmuir probe and a catalytic probe (Babic, Poberaj, & Mozetic, 2001; Poberaj, Mozetic, & Babic, 2002; Vesel & Mozetic, 2001). The Langmuir probe was made from metal rods with the diameter of 1.2 mm, while the catalytic probe was made from a nickel catalyst. The electron temperature of about 3 eV was obtained. By oxygen system an ion density of the order $10^{15}\ m^{-3}$ and neutral atoms of the order $10^{21}\ m^{-3}$, while by NH_3 plasma the electron density of order $10^{16}\ m^{-3}$ was obtained.

Table 1
Sample notation, according to the used treatment procedures. Sample names are composed of the combined first letters of the used treatment procedures in the chronological order as performed (A – alkaline treatment, OP – oxygen plasma treatment, S – silver treatment, NP – ammonium plasma treatment and U – untreated sample).

Sample name	Treatment used			
	Alkaline treatment	Silver treatment	Plasma treatment	
			Oxygen	Ammonium
Two-step pathway				
U				
A	✓			
OP			✓	
AS	✓	✓		
OPS		✓	✓	
One-step pathway				
NP				✓

The sample notations, according to the used treatment procedure are listed in Table 1.

2.3. Methods

2.3.1. Determination of elemental surface chemical composition

The effects of plasma surface modifications were evaluated by studying elemental surface chemical composition with XPS (TFA XPS Physical Electronics). The samples were excited with monochromatic Al $K_{\alpha 1,2}$ radiation at 1486.6 eV over an area of 400 μm^2. Photoelectrons were detected with a hemispherical analyzer positioned at an angle of 45° with respect to the normal of the sample surface. XPS survey spectra were measured at pass energy of 187 eV using an energy step of 0.4 eV. An additional electron gun was used for surface neutralization during XPS measurements. The measured spectra were analyzed using MultiPak v7.3.1 software from Physical Electronics, which was supplied with the spectrometer.

2.3.2. Morphology investigation

To observe possible changes in material surface morphology after different treatment methods were applied, scanning electron microscopy was used. Prior to imaging several single fibers were withdrawn from all samples and pressed on a double-sided adhesive carbon tape (SPI Supplies, USA) respectively. Micrographs were taken using a field emission scanning electron microscope (FE-SEM, Supra 35 VP, Carl Zeiss, Germany) operated at 1 keV. Samples were sputtered with Au/Pd with an 10 nm thick cover. Micrograph results are presented as a secondary electron images (SEI).

2.3.3. Determination of silver surface concentration

For the determination of silver concentration on the viscose nonwoven, the sample was weighted (approximately 0.5 g). The digestion of sample was made in 20 mL of HNO_3 with heating at slight boiling temperature for 2 h. The cold solution was quantitatively transferred in 100 mL flask and it was supplement to sign with distilled water. The digestions of each sample were performed in three parallels. Before the determination of the silver amount on the atomic absorption spectrophotometer, the samples were filtered with Rotilabo®-syringe PTFE filters (Carl Roth, Germany) with pore size 0.45 μm.

2.3.4. In vitro silver release studies

In vitro release studies were used for evaluation of the silver attachment. The dissolution testing was performed using static diffusion cells, according to Franz (1975). Milli-Q water with a maintained constant temperature of 37 °C during the experiment was used for the testing. The temperature was held constant by stirring the thermostatic water around the Franz's diffusion cell. The Ag release from viscose samples with size 1 cm^2 was determined after 24 h as Ag concentration in milli-Q solution using atomic absorption spectroscopy (AAS). All in vitro release studies were performed in 2 parallels. Working standard solutions were prepared in order to prepare the calibration line by dilution of a stock silver standard solution (500 mg/L) in water with 1% (v/v) HNO_3. An atomic absorption spectrometer (PerkinElmer 1100B) equipped with an air-acetylene burner and silver hollow cathode lamp operating at 5 mA was used for determining silver without background correction. The operating conditions were as follows: wavelength: 328.1 nm, band pass: 0.7 nm, flow rate of acetylene: 2.5 L/min, and the flow-rate of air: 8 L/min. All measurements on AAS were performed in 3 parallels.

2.3.5. Hydrophilicity determination

The modified Washburn or capillary-rise method was used for determining the hydrophilicity of porous solid samples. The fabric samples were cut into rectangular pieces (2 cm × 5 cm) and hung up onto sample holder in the Tensiometer Krüss K12 apparatus. The experimental technique based on measuring the samples' weight gain due to liquid penetration as a function of time (Grundke, Boerner, & Jacobasch, 1991; Grundke et al., 1996; Troger, Lunkwitz, Grundke, & Burger, 1998). The evaluation of the measured data is based on modifications of the Washburn equation for a single capillary (Washburn, 1921), which arises from the combination of the expression for the Laplace pressure and the Hagen–Poiseuille equation for steady flow conditions (Grundke, Boerner, & Jacobasch, 1991) as:

$$\gamma_l \cos\theta = \frac{2}{A^2 r}\frac{\mu}{\rho^2}\frac{m}{t} \quad (1)$$

where γ_l is the liquid surface tension, θ is the solid/liquid contact angle, A is the cross-sectional area and r is the radius of the capillary, η is the liquid viscosity, ρ is the liquid density, m is the weight of the liquid that penetrates into the sample capillary, and t is the penetration time.

In the case of fiber samples, the geometry of the capillary system is unknown. Therefore, the unknown factor $(2/A^2 r)$ can be replaced by $1/C$ and determined assuming the capillary radius r_c and a corresponding number of capillaries n_c as:

$$C = \frac{\pi^2}{2} r_c^5 n_c^2 \quad (2)$$

Using n-heptane, complete wetting is assumed resulting in $\cos\theta = 1$. The C can then be calculated as:

$$C = \frac{\mu}{\gamma_l \rho^2}\frac{m^2}{t} \quad (3)$$

Measuring the weight increase during liquid penetration, the contact angle can be determined as:

$$\cos\theta = \frac{1}{C\gamma_l}\frac{\mu}{\rho^2}\frac{m^2}{t} \quad (4)$$

2.3.6. Antimicrobial testing

The general method described in 'AATCC Test Method 100-1999 (American Association of Textile and Colorists, 1999), Antibacterial Finishes on Textile Materials: Assessment of' was used for determination the qualitative and quantitative antibacterial tendencies of the investigated materials. The four challenging bacterial species used in the 'AATCC Test Method 100-1999, Antibacterial Finishes on Textile Materials: Assessment of', were used throughout: *Staphylococcus aureus*, *Escherichia coli*, *Enterococcus faecalis*, and *Pseudomonas aeruginosa* (American Association of Textile and Colorists, 1999). Before each assay, the test bacteria were incubated in either a trypticase soy broth (TSB, BBL® No. 11768 trypticase soy broth) or on trypticase soy agar slants (TSA, BBL® No. 11768 trypticase soy broth, and 2.0% agar) at 37 ± 2 °C for 1–3 days, before being used to inoculate the broth's (TSB) cultures for testing. The inoculated broth cultures were incubated at 37 ± 2 °C and stored at 5 ± 1 °C. Standardized density of bacteria ((1–2) × 10^5 CFU/mL) was used for the challenge inoculation. For each sample's replicate, 1.0 ± 0.1 mL of inoculum was dispersed over the samples (0.1 g), inoculated at 37 ± 2 °C for 24 h, before being assayed for bacterial population density, or were immediately assayed for bacterial population density as the zero-time population density. The bacterial population densities were determined by first extracting the bacteria from the sample by adding 100 mL of diluent to each jar, and then shaking the jars on a table top shaker for 1 min. Then the aliquots were removed and plated directly into petri dishes or further diluted, before being plated. The percentage reduction of bacteria by the samples was determined as:

$$R = 100 \times \frac{B - A}{B} \quad (5)$$

where R is the reduction (%), A is the number of bacteria recovered from the inoculated test specimen swatches in the jar, incubated over the desired contact period (24 h), B is the number of bacteria recovered from inoculated test specimen swatches in the jar immediately after inoculation ("0" contact time).

No antibiotics were used and incubation was at 37 ± 2 °C for 24 h before counting the plates.

3. Results

3.1. Elemental surface chemical compositions

XPS analysis was used to study the binding energy of the C1s and N1s photoelectrons of surface groups on samples treated by the used treatment procedures. The obtained spectra are presented in Fig. 2(a)–(c) along with the calculated elemental surface chemical compositions (d).

Each monosaccharide unit contains five carbon atoms linked to one of oxygen and another carbon linked to two oxygen atoms. Thus, one expects a curve-resolved XPS C1s signal to consist of only two peaks (C2 and C3). The oxygen to carbon ratio for the pure cellulose is expected to be 0:83 (Beamson & Briggs, 1992). However, the same ratio determined for the untreated cellulose material used in this study, was found to be 0:73 (see Fig. 1d).

The alkaline treatment increased the carbon concentration followed by O/C ratio decrease. A decrease in carbon concentration and an increase in the amount of oxygen followed by O/C ratio rise was evident by oxygen plasma treated sample. An increase in concentration of surface nitrogen was provided by NH_3 plasma treatment.

3.2. Surface morphology

Scanning electron microscope was used for imaging of cellulose fine structures and surface morphology. The observable effects of different treatments used are presented in Fig. 3.

The micrograph of the untreated viscose fibers (Fig. 3 – U) shows a fiber diameter around 12–15 μm. Examination of SEM micrographs revealed the complexity of the cellulose fiber structure.

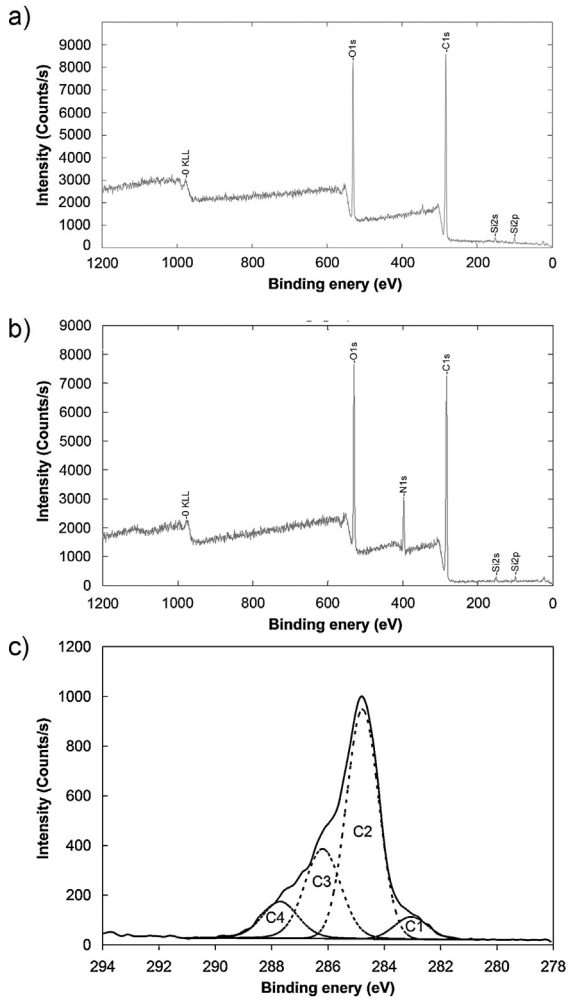

d)

Sample treatment	Surface composition (at. %)				
	C	*O*	*N*	*O/C ratio*	*N/C ratio*
*Theoretical cellulose**	54.5	45.5	0	0.83	0
U - untreated	57.2	42.2	0	0.73	0
A - alkaline treated	62.5	36.2	0	0.57	0
OP - oxygen plasma treated	52.1	47.9	0	0.91	0
NP - NH_3 plasma treated	65.7	22.7	10.4	0.34	0.16

* Beamson & Briggs, 1992)

Fig. 2. Typical XPS spectra for: (a) U – untreated sample and (b) NP – NH_3 plasma treated sample; (c) fitted spectra for sample OP – oxygen plasma treated and (d) calculated contributions of different elements on the surface of the samples are presented. *(Beamson & Briggs, 1992).

Comparing images of treated and untreated fibers exposed the difference in the fiber fine structure and morphology, which occurred due to the used treatment procedures. The intensity of the changes due to different types of fiber treatment varies from no observable morphological changes (sample A) to clearly observable surface alterations (OP, NP). Samples, where the final procedure was the attachment of silver chloride nanoparticles (AS and OPS), exhibit a smoother surface, when compared to the untreated sample. This can be observed especially on the edges of holes and surface bumps, where these appear to be more rounded. Surface parts, where before the treatment different features (like holes, bumps and channels) could be observed, are now covered with thin surface films. The least pronounced effect on the surface is due to the alkaline treatment with sodium hydroxide, which resulted in no observable effect on the surface.

3.3. Surface silver concentration and in vitro silver release evaluation

Determination of the amount of silver in samples AS and OPS showed that all samples exhibited a concentration above the threshold, necessary for the antimicrobial effect (0.060 mg/g) (Hribernik, Pivec, Kurečič, Kolar, & Stana-Kleinschek, 2012). The silver concentration was 0.089 ± 0.02 mg/g and 0.132 ± 0.02 mg/g, respectively for samples AS and OPS.

The efficiency of silver chloride binding by samples treated via two-step pathway (AS and OPS) was evaluated with in vitro silver release testing. The silver release profile of the two mentioned samples was monitored with Franz diffusion cells. The amount of silver released into milli-Q water was determined as silver concentration with the AAS, which showed a concentration below the detection limit (LOD) with AAS, which means a concentration less than 0.05 mg/L.

3.4. Hydrophilic properties

The results of wetting rise curves, depending on used treatments, are presented in Fig. 4. The curves present the weight gained due to water penetration as a function of time. Each curve in the diagram presents the average value of 10 parallel measurements.

The lowest wetting rate was observed as expected by untreated cellulose, while the highest was determined for the oxygen plasma treated samples. Samples treated with ammonium plasma sorbed water with the same rate as oxygen plasma treated samples. Both samples with bound silver chloride exhibit the same wetting rate.

The plateau region of water sorption for the untreated samples was observed after 100 s. Within the first 30 s untreated samples were able to absorb 0.6 g of water. Although were the oxygen plasma treated samples able to absorb the highest amount of water (i.e. 2.5 g), no significant differences in water uptake amount could

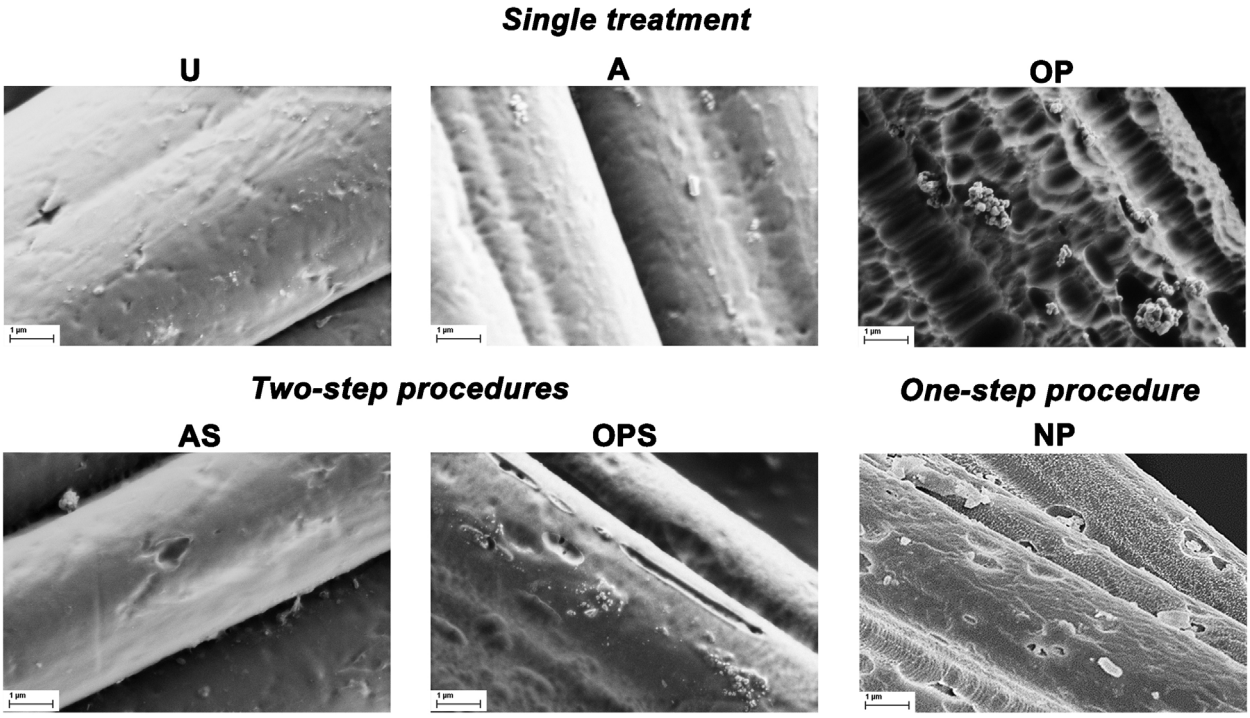

Fig. 3. SEM images of cellulose samples depending on the used treatments: U – untreated; A – alkaline treated; OP – oxygen plasma treated; AS – alkaline and silver treated; OPS – oxygen plasma and silver treated; NP – ammonium plasma treated.

be observed after 13 s, were the plateau was reached for this type of samples. Ammonium treated samples were able to absorb the final amount of water two times faster, when compared to oxygen plasma treated samples, while the absolute value of the absorbed water was twice as low. Comparing the silver chloride treated samples, no significant differences in water uptake amount could be observed (i.e. 0.95 g) after 13 s, where the plateau was reached.

Contact angles for the water/solid pairs were calculated using Eq. (4) and m^2/t values obtained from wetting rise curves are presented in Fig. 5. Shown results are the average of 10 measurements performed on each of the samples.

The highest water contact angle was observed for the untreated sample. All performed treatments resulted in improved hydrophilicity, most significantly for the ammonium and oxygen plasma treated samples, which experienced an contact angle decrease of 66 and 70%, respectively. The attachment of silver chloride nanoparticles in the two-step preparation procedure reversed the improved hydrophilic character, obtained either due to alkaline or plasma treatment. Contact angles for the mentioned samples increased for 26–141%.

3.5. Antimicrobial properties

Antimicrobial testing was performed for the untreated sample (U) and compared to the results of samples, treated in the different described ways. Two Gram-positive (i.e. *S. aureus* and *E. faecalis*) and two Gram-negative (i.e. *E. coli* and *P. aeruginosa*) bacteria were used. The selected bacteria are increasingly recognized as the most dangerous (and common) opportunistic pathogens with clinical relevance. Another important factor, which led to their choice for testing, is the progressively increasing antibiotic resistance in clinical isolates. The antimicrobial activity of tested samples, presented as a reduction (R) of bacteria, is listed in Table 2.

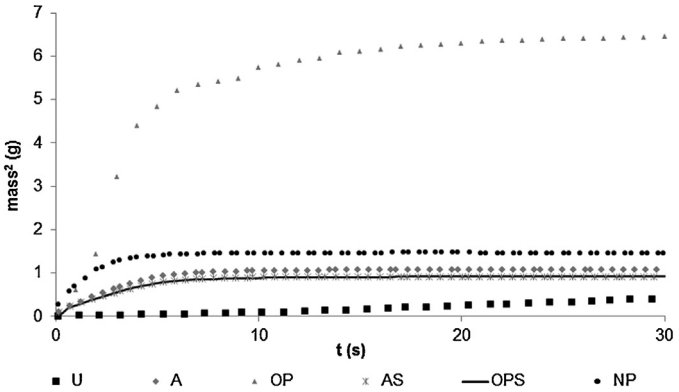

Fig. 4. Wetting rise curves of water as a function of time measured for different treated samples: U – untreated; A – alkaline treated; OP – oxygen plasma treated; AS – alkaline and silver treated (two-step pathway); OPS – oxygen plasma and silver treated (two-step pathway); NP – ammonium plasma treated (one-step pathway).

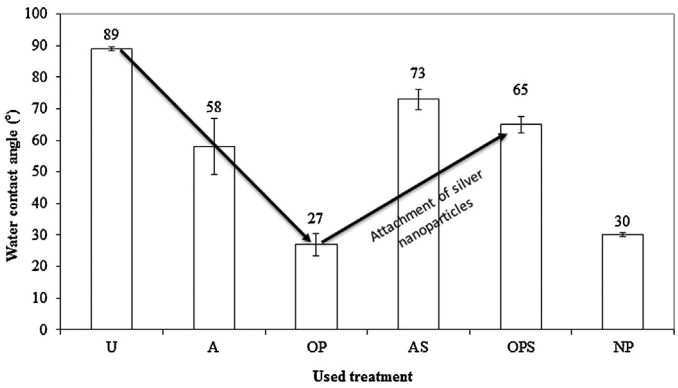

Fig. 5. Water contact angles of cellulose samples depending on used treatments: U – untreated, A – alkaline treated; OP – oxygen plasma treated; AS – alkaline and silver treated (two-step pathway); OPS – oxygen plasma and silver treated (two-step pathway); NP – ammonium plasma treated (one-step pathway).

Table 2
Reduction *R* (%) of bacteria for cellulose samples, depending on treatment used: U – untreated, A – alkaline treated; OP – oxygen plasma treated; AS – alkaline and silver treated (two-step pathway); OPS – oxygen plasma and silver treated (two-step pathway); NP – ammonium plasma treated (one-step pathway).

Sample treatment	Reduction *R* (%) of the bacterial culture			
	S. aureus	*E. coli*	*E. faecalis*	*P. aeruginosa*
U	No reduction	No reduction	77	No reduction
A	100	No reduction	100	No reduction
OP	100	No reduction	100	No reduction
AS	98	100	100	100
OPS	90	100	100	100
NP	100	No reduction	81	No reduction

The results for the untreated samples, as shown in Table 2, indicate no reduction for *S. aureus*, *E. coli* and *P. Aeruginosa*, while a significant reduction (77%) was observed for *E. faecalis*. This result was rather unpredictable, although the percentage does not count as antimicrobial activity; the noticeable antimicrobial challenge delivering a higher value (Fras-Zemljic, Kokol, & Cakara, 2011).

The alkaline treated (A) and both plasma treated samples (OP and NP) resulted in similar antimicrobial activities. Comparison with the untreated sample (U) reveals a broader antibacterial spectrum since the reduction on both gram-positive bacteria was evidenced.

As expected, the samples with incorporated silver chloride resulted in full reduction of all tested bacteria.

4. Discussion

4.1. Treatment vs. chemical composition

The differences in O/C ratio as obtained by untreated sample compared to pure cellulose may occur due to contaminants present in the measured sample (Carlsson & Strom, 1991).

An increased carbon amount by alkaline treated sample should be representative of ubiquitous carbon-based contaminants in air-exposed surfaces during drying (Johansson & Campbell, 2004).

By oxygen plasma treated cellulose samples the oxidation caused an increase in the amount of oxygen followed by O/C ratio rise. During plasma treatment different radicals are formed, which react with oxygen resulting in oxygen-containing functional groups i.e. carbonyl and carboxyl. The latter can be observed as changes in C3 and C4 peaks in C1s (Belgacem, Czeremuszkin, Sapieha, & Gandini, 1995; Sapieha, Verreault, Klemberg-Sapieha, Sacher, & Wertheimer, 1990).

On exposure to ammonium plasma, the incorporation of N-containing functional groups such as amine, imine, amide and nitrile on different materials has been reported (Gancarz, Poźniak, & Bryjak, 2000; Salerno et al., 2009). Regarding the mentioned studies and the obtained results as shown in Fig. 2d, one can speculate that the following events can take place during ammonia treatment. First, the longest periods of cellulose exposure to ammonium plasma can result in cellulose chain scission. Second, due to this event, reactive chain ends become available for interaction with the nitrogen atoms, present in ammonium plasma. In this case, chemical moieties containing both oxygen and nitrogen atoms with molecular formulas of the type $-C_xH_yON$ and $-C_xH_yO_2N$ can be generated.

4.2. Sample morphology vs. hydrophilicity

Comparing the untreated sample (U) and the samples treated with different procedures revealed a high influence of the used treatment on the surface morphology (Fig. 3). The most observable changes appear for samples (OP and NP), where plasma treatment was the only used procedure. Plasma treatment evidently does not result only in surface functionalization, but causes additional surface etching. The result of the latter is that both plasma treated samples exhibit holes (craters) on the surface in diameters of up to a couple hundred nm (Fig. 3). These changes in the surface topography are mostly caused by chemical and physical erosion due to atoms and ions in the plasma (Vesel, Junkar, Cvelbar, Kovac, & Mozetic, 2008). Due to this effect their surface roughness was increased, which can contribute to higher wettability and hence hydrophilicity for samples treated in such a way. In fact, samples where plasma was the final treatment procedure (OP and NP) exhibit the best hydrophilic properties (Fig. 5).

Another observable effect is due to the attachment of silver chloride nanoparticles. Their size was determined in one of our previous studies (Pivec et al., 2013), where it was found (using three different methods) to be in the range from 100 nm to 500 nm. The same size was also reported by other researchers (Tomsic et al., 2009). Silver chloride nanoparticles were attached to the surface using a specially designed sol-gel procedure, which enables the silver chloride nanoparticles to stick to the surface on a prolonged basis. While the mentioned effect leads to a safe antimicrobial activity of the prepared materials, it also renders the sample surface less rough. Safe silver release means preserved antimicrobial activity, while the cytotoxic effects are avoided by diminishing the silver release. The latter is the direct consequence of the used procedure, where the fiber surface is first covered with a thin layer of the sol-gel solution, which is evenly distributed over the surface; this is then transformed to the gel state and the result is a smoother surface (Fig. 3). Smoother surface means that the improved hydrophilicity acquired by the treatment procedures (either the alkaline treatment for the samples AS or the plasma treatment for the sample OPS), is reversed to a certain degree (Fig. 5).

The least pronounced surface changes can be observed after the alkaline treatment (A). The reason for that is probably the fact that NaOH is added to the surface from a solution, where the NaOH molecules are fully dispersed in water. After dipping of viscose into this solution, these get attached to the surface as lone molecules, and therefore leave no measurable features on the surface (Fig. 3). Although the effect of this treatment cannot be identified from the SEM micrographs, their influence can be seen from the increased hydrophilicity after the treatment. In contrast to the plasma treated samples, where the improved hydrophilic properties are most likely connected with the increase surface roughness measured on the nano- or macro-scale, are the changes due to the alkaline treatment macroscopic. Increased distance between individual fibers (destruction of the intermolecular hydrogen bonds between cellulose chains), increased surface area due to macroscopic cracks in the fiber are just a couple of the phenomena, which contribute to the improved hydrophilicity due to the alkaline treatment (Krässig, 1993; Roy, Semsarilar, Guthrie, & Perrier, 2009).

4.3. Modification vs. hydrophilicity

Alkaline treatment (A) caused structural re-organisation (Smole et al., 2003) resulting in accessibility of carboxyl groups located in inner regions. The increased hydrophilicity occurred due to interaction of carboxyl groups with water (Persin, Stenius, & Stana-Kleinschek, 2011) as evidenced by water contact angle decrease. Oxygen plasma (OP) resulted in significant increase of hydrophilicity due to activation of remaining hydroxyl groups as well due to introduction of new functionalities that interact with water. The NH_3 plasma (NP) was used for introduction of amino groups onto the cellulose surface and therefore changed its polarity and reactivity resulting in improved wettability. While a clear increase in the hydrophilic character could be observed due to plasma treatment (either oxygen–OP or ammonium–NP), this effect was somewhat

reversed as the result of the silver chloride attachment, as described in the previous section. Apart from the mentioned mechanism of the decrease in hydrophilicity, this could be lowered also due to introduction of nonpolar moieties, which are present in the used sol-gel binder that covered (or even reacts with) the freshly formed, plasma induced, and hydrophilic surface functional groups.

4.4. Hydrophilicity vs. antimicrobial activity

Mostly the antibacterial activity is connected with specific functional groups and moieties. Oxygen plasma treated samples (OP) compared to alkaline treated (A) provide excellent hydrophilicity, while a similar and not sufficient antimicrobial effect was achieved since the reduction only on both Gram-positive bacteria was evident. Attaching the silver chloride nanoparticles after the alkaline or oxygen plasma treated samples (two-step pathway—samples AS and OPS) resulted in a significant antimicrobial activity. Independent of the initial silver concentration after the attachment, both samples showed no measurable silver release, providing a safe antimicrobial activity. Safety is assured by diminishing the release of silver, which is connected with the possible cytocompatibility issues.

Although both plasma treatments (OP and NP) caused almost similar improvement in hydrophilicity, the antimicrobial activity was more pronounced using the oxygen plasma. The latter could be explained by changed, i.e. more improved hydrophilic properties by OP samples. The connection of altered antimicrobial activity due to improved hydrophilic properties was also considered by other researchers (Bruggisser, 2005; Fras Zemljic, Sauperl, But, Zabret, & Lusicky, 2011; Mi et al., 2001; Ovington, 2001, 2007). Bacteria exist over a wide range of shapes, ranging from rods – bacillus to spheres – cocci and to spirals, which differ in dimensions and exhibit shape specific properties. *E. faecalis* and *S. aureus* belong to spherically-shaped bacteria (diameter of 0.5–1.0 μm), while *E. coli* and *P. aeruginosa* belong to rod shaped bacteria (i.e. *E. coli* width: 1–2 μm, length: 3–30 μm). Considering the mentioned, spherical shaped bacteria having smaller diameters, could more easily penetrate into the porous samples, especially the hydrophilic ones (Bruggisser, 2005; Mi et al., 2001; Ovington, 2001, 2007). According to the mentioned facts, bacteria could be adsorbed onto the modified sample surface with an improved hydrophilic character, resulting in apparent antimicrobial activity.

In addition to these results we can say that both plasma treated samples (OP and NP samples) exhibit a satisfactory hydrophilicity, while their antibacterial activities were limited to only two potentially pathogenic bacteria. The attachment of silver nanoparticles (in the two-step pathway—samples OPS and AS) resulted in a desired antimicrobial activity against all four common pathogenic bacteria, but it simultaneously negatively affected the obtained hydrophilicity, which in turn can decrease the achieved optimal healing conditions.

4.5. Cytocompatibility vs. treatment

Silver release from prepared materials onto the skin can have apart from the desired antimicrobial effects, also some undesired effects. The latter can be associated with silvers possible cytotoxicity (AshaRani et al., 2008; Kim, Yang, & Ryu, 2010; Lina et al., 2010). To minimize or even prevent the release, which is the cause for this effect, we bound the antimicrobial silver chloride nanoparticles in the two-step pathway procedure via a sol–gel based process (Pivec et al., 2012). According to Burd et al., silver skin concentrations above 2 mg/L (Burd et al., 2007) can result in a cytotoxic effect. Obtained concentrations of released silver from AS and OPS samples indicated a negligible silver release, therefore these samples could be considered safe.

As an alternative method to obtain antimicrobial activity of the prepared materials, we treated our samples using oxygen and/or nitrogen gas plasma treatment. Such treatment methods are known as one of the strategies for enhancing surface properties, including enrichment with newly formed functional groups and an enhanced cell proliferation (Coen, Lehmann, Groening, & Schlapbach, 2003; Kim, Kang, Huh, & Yoon, 2000). Using plasma technology the formation of new functional groups, such as hydroxyl (—OH), amine (—NH_x), methyl (—CH_3) sulphate (—SO_4) or carboxylic (—COOH) was reported, resulting in improved biocompatibility/hemocompatibility of the treated surface (Sperling, Schweiss, Streller, & Werner, 2005; Tzoneva et al., 2008).

Using the mentioned plasma treatment, we additionally improve the surface wettability, which is believed to be one of the most important parameters, affecting the biological tissue response to a material in contact. Junkar, Cvelbar, and Lehocky (2011) have shown that RF oxygen and nitrogen plasma treatment improve proliferation of fibroblasts as well as endothelia cells (Chen, Zamora, Som, Pena, & Osaki, 2003; Ramires, Mirenghi, Romano, Palumbo, & Nicolardi, 2000). Improved proliferation of cells was reported to be attributed to newly formed functional groups (oxygen- and nitrogen-based) that were introduced using the plasma treatment. The plasma treatment resulted in an improved hydrophilic character (Chen, Zamora, Som, Pena, & Osaki, 2003; Junkar, Cvelbar, & Lehocky, 2011). According to Dalby et al., surface morphology has to be considered simultaneously with the hydrophilic/hydrophobic character of the samples, when assessing the biological response of tissue to biomaterials, resulting in the materials' cytocompatiblity (Dalby, Riehle, Johnstone, Affrossman, & Curtis, 2002).

The cell attachment and spreading may be important factors in developing wound dressing material therefore the cytotoxicity and cytocompatibility tests are useful in design and tailoring of matrices for wound healing management. Ramires, Mirenghi, Romano, Palumbo, and Nicolardi (2000) verified the effect of O_2 and NH_3 plasma treated PET surfaces in regard of cytotoxicity and cytocompatibility. Their results show that plasma treatment of PET samples did not result in an increased toxicity on human umbilical vein endothelial cells. In fact, the cytocompatibility tests revealed an increase in cell growth by NH_3 plasma treated PET sample. Wang et al. (2004) evaluated the cell affinity of the oxygen-treated poly-(lactide-co-glycolide) (PLGA) films under dynamic conditions. The results evidenced that improved cell adhesion was more contributed to the surface chemistry then to surface morphology. Namely, for the sample treated with O_2-plasma for 10 min, the percentage of adherent cells was the highest compared to the sample treated for 20 min and exhibiting the roughest surface. Jeong et al. (2009) investigated the cellular responses of the O_2 and CH_4 plasma treated silk fibroin nanofibers using normal human keratinocytes and fibroblasts which were aimed at generating skin tissue. They found that O_2-treated sample showed the highest cellular activities as a consequence of increased hydrophilicity.

4.6. Two-step procedure vs. one-step procedure

The focus of the two-step pathway used in this study was to define the optimal combination of two known effective treatments, used to separately obtain optimal hydrophilic properties and a desired antimicrobial activity. The hydrophilicity and antimicrobial properties obtained by two-step pathway were compared to the properties obtained by one-step pathway, which was used to simultaneously provide both desired effects.

Comparing both treatment pathways, the one-step procedure provides improved hydrophilicity, while a broader antimicrobial activity was achieved by the two-step procedure. At this point it is necessary to state that the two-step procedure takes more time to yield the desired materials. The two-step pathway enables the

production of highly effective materials against pathologic bacteria, but does not provide the proper hydrophilic properties, which are required for optimal wound healing. Since both pathway procedures were able to provide antimicrobial properties, the deciding factor in developing wound dressings could be sorption management. More importantly, we can make a reasonable assumption that the wound care market will rise to more than 20 billion $ within the next two years; as well it is expected to grow for nearly 7% per year (Information, 2011). It was also estimated that the costs of products for the management of chronic wounds at home takes ups to 5% of the total cost for nurse home visits (Nametka & Gibbins, 2002). Decreasing the production costs by introducing rather one-step procedure could therefore be a viable strategy to contain the expanding costs of the health care agencies.

5. Conclusions

The goal of the present study was to compare two pathways for achieving a safe and efficient wound treatment. Viscose nonwoven was chosen as the base material for the functionalization procedures. The two-step pathway used two separate processes to achieve the desired properties, namely the optimal hydrophilicity and antimicrobial activity. In the first step either an alkaline (sample AS) or oxygen plasma treatment procedure (OPS) is used, while silver is the lone source of the antimicrobial activity of these samples. The second pathway is another step ahead due to the simultaneous achievement of both desired properties by only one treatment procedure, namely the ammonium plasma–NP sample.

When comparing the two used pathways regarding their antimicrobial activity, we can see that the two-step procedure exhibits superior results. Silver as a broad spectrum antibacterial agent is capable of fully destroying all of the tested bacteria. Although attachment of the silver chloride nanoparticles led to an efficient antibacterial activity, it weakened the effects of the improved hydrophilicity gained by alkaline (sample AS) and plasma treatment (OPS). Ammonium plasma treatment (sample NP) on the other hand, as a one-step approach, significantly improved hydrophilicity (see Figs. 4 and 5), but could not provide the desired antimicrobial activity on all four of the used bacteria.

Finally, the decision of using the appropriate dressing should be therefore based on the assessment of the three key wound parameters, which change for different wound types—healing, exudation and infection. Materials prepared by the one-step procedure with superior hydrophilicity and a limited antimicrobial activity could therefore be the first choice for strongly exudating wounds, where the antimicrobial activity can be more used as a preventive measure. One the other hand materials prepared by the two-step procedure with a highly effective and safe broad spectrum antimicrobial activity but with lower hydrophilicity could be more useful for wounds with less exudation, but high risk of infection.

Further systematic research of one-step pathway toward more efficient antimicrobial activity in the direction of Gram-negative bacteria is needed for yielding commercial interesting wound dressing material.

Acknowledgement

The authors acknowledge the financial support from the Ministry of Education, Science, Culture and Sport of the Republic of Slovenia through the contract No. 3211-10-000057 (Center of Excellence for Polymer Materials and Technologies).

References

American Association of Textile and Colorists. (1999). *Antibacterial finishes on textile materials: Assessment of*. Research Triangle Park, NC: AATCC.

AshaRani, P. V., Low Kah Mun, G., Hande, M. P., & Valiyaveettil, S. (2008). Cytotoxicity and genotoxicity of silver nanoparticles in human cells. *ACS Nano*, *3*(2), 279–290.

Babic, D., Poberaj, I., & Mozetic, M. (2001). Fiber optic catalytic probe for weakly ionized oxygen plasma characterization. *Review of Scientific Instruments*, *72*(11), 4110–4114.

Baohua, L., Hu, J., & Meng, Q. (2009). Nonwoven supported temperature-sensitive poly(N-isopropylacrylamide)/polyurethane copolymer hydrogel with antibacterial activity. *Journal of Biomedical Materials Research Part B*, *89*(1), 1–8.

Beamson, G., & Briggs, D. (1992). *High resolution XPS of organic polymers: The Scienta ESCA300 database*. Chichester England/New York: Wiley.

Belgacem, M. N., Czeremuszkin, G., Sapieha, S., & Gandini, A. (1995). Surface characterization of cellulose fibres by XPS and inverse gas chromatography. *Cellulose*, *2*(3), 145–157.

Breitwieser, D., Moghaddam, M. M., Spirk, S., Baghbanzadeh, M., Pivec, T., Fasl, H., et al. In-situ preparation and characterization of silver nanocomposites on cellulosic fibers—Microwave vs. conventional heating. *Carbohydrate Polymers*, in press

Breitwieser, D., Spirk, S., Fasl, H., Ehmann, H. M. A., Chemelli, A., Reichel, V. E., et al. Design of simultaneous antimicrobial and anticoagulant surfaces based on nanoparticles and polysaccharides. *Journal of Materials Chemistry B*, in press

Bruggisser, R. (2005). Bacterial and fungal absorption properties of a hydrogel dressing with a superabsorbent polymer core. *Journal of Wound Care*, *14*(9), 438–442.

Burd, A., Kwok, C. H., Hung, S. C., Chan, H. S., Gu, H., Lam, W. K., et al. (2007). A comparative study of the cytotoxicity of silver-based dressings in monolayer cell, tissue explant, and animal models. *Wound Repair and Regeneration*, *15*(1), 94–104.

Cady, N. C., Behnke, J. L., & Strickland, A. D. (2011). Copper-based nanostructured coatings on natural cellulose: Nanocomposites exhibiting rapid and efficient inhibition of a multi-drug resistant wound pathogen, *A. baumannii*, and mammalian cell biocompatibility in vitro. *Advanced Functional Materials*, *21*(13), 2506–2514.

Carlsson, C. M. G., & Strom, G. (1991). Reduction and oxidation of cellulose surfaces by means of cold-plasma. *Langmuir*, *7*(11), 2492–2497.

Chekmareva, I. A. (2002). Experimental study of reparative regeneration processes in the wound treated with bioactive dressings. *Bulletin of Experimental Biology and Medicine*, *133*, 192–195.

Chen, J. P., & Chiang, Y. (2010). Bioactive electrospun silver nanoparticles-containing polyurethane nanofibers as wound dressings. *Journal of Nanoscience and Nanotechnology*, *10*(11), 7560–7564.

Chen, M., Zamora, P. O., Som, P., Pena, L. A., & Osaki, S. (2003). Cell attachment and biocompatibility of polytetrafluoroethylene (PTFE) treated with glow-discharge plasma of mixed ammonia and oxygen. *Journal of Biomaterials Science Polymer Edition*, *14*(9), 917–935.

Coen, M. C., Lehmann, R., Groening, P., & Schlapbach, L. (2003). Modification of the micro- and nanotopography of several polymers by plasma treatments. *Applied Surface Science*, *207*(1–4), 276–286.

Corum, L., Thomas, J. G., Slone, W., Linton, S., Okel, T., & Percival, S. L. (2011). A comparison of the efficacy and sustainability of silver containing wound dressings evaluated with flow cytometry, corrected zone of inhibition and log reduction in-vitro methods. *Wound Repair and Regeneration*, *19*(2), A18.

Dalby, M. J., Riehle, M. O., Johnstone, H., Affrossman, S., & Curtis, A. S. G. (2002). In vitro reaction of endothelial cells to polymer demixed nanotopography. *Biomaterials*, *23*(14), 2945–2954.

Durso, D. F. (1978). *Chemical modification of cellulose—A historical review*. New York: Academic Press.

Eid, K. A., & Azzazy, H. M. (2012). Controlled synthesis and characterization of hollow flower-like silver nanostructures. *International Journal of Nanomedicine*, *7*, 1543–1550.

Esteban-Cubillo, A., Pecharromán, C., Aguilar, E., & Moya, J. (2006). Antibacterial activity of copper monodispersed nanoparticles into sepiolite. *Journal of Materials Science*, *41*(16), 5208–5212.

Fengel, D., & Wegener, G. (1984). *Reactions in alkaline medium*. Berlin, New York: Walter de Gruyter.

Franz, T. J. (1975). Percutaneous absorption on the relevance of in vitro data. *Journal of Investigative Dermatology*, *64*(3), 190–195.

Fras-Zemljic, L., Kokol, V., & Cakara, D. (2011). Antimicrobial and antioxidant properties of chitosan-based viscose fibres enzymatically functionalized with flavonoids. *Textile Research Journal*, *81*, 1532–1540.

Fras Zemljic, L., Sauperl, O., But, I., Zabret, A., & Lusicky, M. (2011). Viscose material functionalized by chitosan as a potential treatment in gynecology. *Textile Research Journal*, *81*(11), 1183–1190.

Fraser, J. F., Cuttle, L., Kempf, M., & Kimble, R. M. (2004). Cytotoxicity of topical antimicrobial agents used in burn wounds in Australasia. *ANZ Journal of Surgery*, *74*(3), 139–142.

Freytag, R., & Donzé, J. J. (1983). *Alkali treatment of cellulose fibres*. New York and Basel: Marcel Deckker Inc.

Gancarz, I., Poźniak, G., & Bryjak, M. (2000). Modification of polysulfone membranes. 3. Effect of nitrogen plasma. *European Polymer Journal*, *36*(8), 1563–1569.

Gilbert, P., & Moore, L. E. (2005). Cationic antiseptics: Diversity of action under a common epithet. *Journal of Applied Microbiology*, *99*(4), 703–715.

Grundke, K., Boerner, M., & Jacobasch, H. J. (1991). Characterization of fillers and fibers by wetting and electrokinetic measurements. *Colloids and Surfaces*, *58*(1–2), 47–59.

Grundke, K., Bogumil, T., Gietzelt, T., Jacobasch, H. J., Kwok, D. Y., & Neumann, A. W. (1996). Wetting measurements on smooth, rough and porous solid surfaces. *Interfaces, Surfactants and Colloids in Engineering*, *101*, 58–68.

Hart, J., Silcock, D., & Gunnigle, S. (2002). The role of oxidised regenerated cellulose/collagen in wound repair: Effects in vitro on fibroblast biology and in vivo in a model of compromised healing. *International Journal of Biochemistry & Cell Biology*, *34*, 1557–1570.

Hengstberger, M., Kaltenecker, O., & Oppermann, W. (1999). Vliesstoffe mit superabsorbierenden Eigenschaften. *Technische Textillien*, *42*, 295–297.

Hribernik, S., Pivec, T., Kurečič, M., Kolar, M., & Stana-Kleinschek, K. (2012). Optimization of the sol–gel-assisted procedure for binding of silver onto modal fibres. In *7th central European conference 2012 fibre-grade polymers* Portorose, Slovenia, (pp. 265–271).

Hyde, K. G., Stewart, S. M., Scarel, G., Parsons, G. N., Shih, C. C., Shis, C. M., et al. (2011). Atomic layer deposition of titanium dioxide on cellulose acetate for enhanced hemostasis. *Biotechnology Journal*, *6*(2), 213–223.

Infante, M. R., Perez, L., Pinazo, A., Clapes, P., Moran, M. C., Angelet, M., et al. (2004). Amino acid-based surfactants. *Comptes Rendus Chimie*, *7*(6–7), 583–592.

Information, K. (2011). *World wound care markets 2011*. Kalorama.

Jeong, L., Yeo, I. S., Kim, H. N., Yoon, Y. I., Jang, D. H., Jung, S. Y., et al. (2009). Plasma-treated silk fibroin nanofibers for skin regeneration. *International Journal of Biological Macromolecules*, *44*(3), 222–228.

Jing, A., Zhang, H., Zhang, J., Zhao, Y., & Yuan, X. (2009). Preparation and antibacterial activity of electrospun chitosan/poly(ethylene oxide) membranes containing silver nanoparticles. *Colloid and Polymer Science*, *287*(12), 1425–1434.

Johansson, L. S., & Campbell, J. M. (2004). Reproducible XPS on biopolymers: Cellulose studies. *Surface and Interface Analysis*, *36*(8), 1018–1022.

Junkar, I., Cvelbar, U., & Lehocky, M. (2011). Plasma treatment of biomedical materials. *Materiali in Tehnologije*, *45*(3), 221–226.

Junping, J., Xin, L., Dequan, Z., & Li, Z. (2010). Doping/dedoping process induced wettability switching of polyaniline-coated conductive textile. *Acta Polymerica Sinica*, *2*, 192–198.

Kim, Y. J., Kang, I. K., Huh, M. W., & Yoon, S. C. (2000). Surface characterization and in vitro blood compatibility of poly(ethylene terephthalate) immobilized with insulin and/or heparin using plasma glow discharge. *Biomaterials*, *21*(2), 121–130.

Kim, Y.-J., Yang, S., & Ryu, J.-C. (2010). Cytotoxicity and genotoxicity of nano-silver in mammalian cell lines. *Molecular & Cellular Toxicology*, *6*(2), 119–125.

Klode, J., Schottler, L., Stoffels, I., Korber, A., Schadendorf, D., & Dissemond, J. (2011). Investigation of adhesion of modern wound dressings: A comparative analysis of 56 different wound dressings. *Journal of the European Academy of Dermatology and Venereology*, *25*(8), 933–939.

Kokura, S., Handa, O., Takagi, T., Ishikawa, T., Naito, Y., & Yoshikawa, T. (2010). Silver nanoparticles as a safe preservative for use in cosmetics. *Nanomedicine*, *6*(4), 570–574.

Kontogiannopoulos, K. N., Assimopoulou, A. N., Tsivintzelis, I., Panayiotou, C., & Papageorgiou, V. P. (2011). Electrospun fiber mats containing shikonin and derivatives with potential biomedical applications. *International Journal of Pharmaceutics*, *409*(1-2), 216–228.

Krässig, H. A. (1993). *Cellulose: Structure, accessibility and reactivity*. Yverdon, Switzerland; Philadelphia: Gordon and Breach Science.

Kuroyanagi, Y., Shiraishi, A., Shirasaki, Y., Nakakita, N., Yasutomi, Y., Takano, Y., et al. (1994). Development of a new wound dressing with antimicrobial delivery capability. *Wound Repair and Regeneration*, *2*(2), 122–129.

Lalani, R., & Liu, L. (2012). Electrospun zwitterionic poly(sulfobetaine methacrylate) for nonadherent, superabsorbent, and antimicrobial wound dressing applications. *Biomacromolecules*, *13*(6), 1853–1863.

Lansdown, A. B. (2002). Silver. I. Its antibacterial properties and mechanism of action. *Journal of Wound Care*, *11*(4), 125–130.

Lee, A. R., & Huang, W. H. (1995). Zinc sulphadiazines: Novel topical antimicrobial agents for burns. *Journal of Pharmacy and Pharmacology*, *47*(6), 503–509.

Lewin, M. (1984). *Bleaching of cellulosic and synthetic fabrics*. New York and Basel: Marcel Dekker Inc.

Wei, L., Tang, J., Zhang, Z., Chen, Y., Zhou, G., & Xi, T. (2010). Investigation of the cytotoxicity mechanism of silver nanoparticles in vitro. *Biomedical Materials*, *5*(4), 044103.

Liu, J., Sonshine, D. A., Shervani, S., & Hurt, R. H. (2010). Controlled release of biologically active silver from nanosilver surfaces. *ACS Nano*, *4*(11), 6903–6913.

Lok, C. N., Ho, C. M., Chen, R., He, Q. Y., Yu, W. Y., Sun, H., et al. (2006). Proteomic analysis of the mode of antibacterial action of silver nanoparticles. *Journal of Proteome Research*, *5*(4), 916–924.

Madhumathi, K., Sudheesh Kumar, P. T., Abhilash, S., Sreeja, V., Tamura, H., Manzoor, K., et al. (2010). Development of novel chitin/nanosilver composite scaffolds for wound dressing applications. *Journal of Materials Science-materials in Medicine*, *21*(2), 807–813.

Malmsten, M. (2011). Antimicrobial and antiviral hydrogels. *Soft Matter*, *7*(19), 8725–8736.

Mi, F.-L., Shyu, S.-S., Wu, Y.-B., Lee, S.-T., Shyong, J.-Y., & Huang, R.-N. (2001). Fabrication and characterization of a sponge-like asymmetric chitosan membrane as a wound dressing. *Biomaterials*, *22*(2), 165–173.

Mikhaylova, A., Liesenfeld, B., Moore, D., Toreki, W., Vella, J., Batich, C., et al. (2011). Preclinical evaluation of antimicrobial efficacy and biocompatibility of a novel bacterial barrier dressing. *Wounds*, *23*(2), 24–31.

Nametka, M., & Gibbins, B. (2002). Silver antimicrobial absorbent wound dressing can contribute to cost control in home care. In *17th annual clinical symposium on advances in skin and wound care* Dallas, TX,

Ovington, L. G. (2001). Battling bacteria in wound care. *Home Healthcare Nurse*, *19*(10), 622–630 (quiz 630–1).

Ovington, L. G. (2007). Advances in wound dressings. *Clinics in Dermatology*, *25*(1), 33–38.

Percival, S. L., Bowler, P. G., & Russell, D. (2005). Bacterial resistance to silver in wound care. *Journal of Hospital Infection*, *60*(1), 1–7.

Persin, Z., Stenius, P., & Stana-Kleinschek, K. (2011). Estimation of the surface energy of chemically and oxygen plasma-treated regenerated cellulosic fabrics using various calculation models. *Textile Research Journal*, *81*(16), 1673–1685.

Pivec, T., Persin, Z., Hribernik, S., Maver, T., Kolar, M., & Stana-Kleinschek, K. (2012). Binding silver nano-particles onto viscose non-woven using different commercial sol-gel procedures. *Materiali in Tehnologije*, *46*(1), 75–80.

Pivec, T., Persin, Z., Kolar, M., Maver, T., Dobaj, A., Vesel, A., et al. (2013). Modification of cellulose non-woven for preparation of modern wound dressings. *Textile Research Journal*, in press.

Poberaj, I., Mozetic, M., & Babic, D. (2002). Comparison of fiber optics and standard nickel catalytic probes for determination of neutral oxygen atoms concentration. *Journal of Vacuum Science & Technology A-Vacuum Surfaces and Films*, *20*(1), 189–193.

Ramires, P. A., Mirenghi, L., Romano, A. R., Palumbo, F., & Nicolardi, G. (2000). Plasma-treated PET surfaces improve the biocompatibility of human endothelial cells. *Journal of Biomedical Materials Research*, *51*(3), 535–539.

Reichel, V. (2012). *Functionalisation of cellulose acetate surfaces for removal the of endocrine disruption compounds. Diploma Thesis*. Department of Colloid Science: University of Graz.

Robb, E. C., & Nathan, P. (1981). Control of experimental burn wound infections: Comparative delivery of the antimicrobial agent (silver sulfadiazine) either from a cream base or from a solid synthetic dressing. *Journal of Trauma*, *21*(10), 889–893.

Rowe, R. C., Sheskey, P. J., & Quinn, M. E. (2009). Handbook of pharmaceutical excipients. In R. C. Rowe (Ed.), *Alginic acid* (pp. 48–51). London, UK: Pharmaceutical Pr.

Roy, D., Semsarilar, M., Guthrie, J. T., & Perrier, S. (2009). Cellulose modification by polymer grafting: A review. *Chemical Society Reviews*, *38*(7), 2046–2064.

Salerno, S., Piscioneri, A., Laera, S., Morelli, S., Favia, P., Bader, A., et al. (2009). Improved functions of human hepatocytes on NH3 plasma-grafted PEEK-WC-PU membranes. *Biomaterials*, *30*(26), 4348–4356.

Sapieha, S., Verreault, M., Klemberg-Sapieha, J. E., Sacher, E., & Wertheimer, M. R. (1990). X-ray photoelectron study of the plasma fluorination of lignocellulose. *Applied Surface Science*, *44*(2), 165–169.

Seetharaman, S., Natesan, S., Stowers, R. S., Mullens, C., Baer, D. G., Suggs, L. J., et al. (2011). A PEGylated fibrin-based wound dressing with antimicrobial and angiogenic activity. *Acta Biomaterialia*, *7*(7), 2787–2796.

Smole, M. S., Persin, Z., Kreze, T., Kleinschek, K. S., Ribitsch, V., & Neumayer, S. (2003). X-ray study of pre-treated regenerated cellulose fibres. *Materials Research Innovations*, *7*(5), 275–282.

Sperling, C., Schweiss, R. B., Streller, U., & Werner, C. (2005). In vitro hemocompatibility of self-assembled monolayers displaying various functional groups. *Biomaterials*, *26*(33), 6547–6557.

Thomas, S. (2008). A review of the physical, biological and clinical properties of a bacterial cellulose wound dressing. *Journal of Wound Care*, *17*(8), 349–352.

Tomsic, B., Simoncic, B., Orel, B., Zerjav, M., Schroers, H., Simoncic, A., et al. (2009). Antimicrobial activity of AgCl embedded in a silica matrix on cotton fabric. *Carbohydrate Polymers*, *75*(4), 618–626.

Troger, J., Lunkwitz, K., Grundke, K., & Burger, W. (1998). Determination of the surface tension of microporous membranes using wetting kinetics measurements. *Colloids and Surfaces A-Physicochemical and Engineering Aspects*, *134*(3), 299–304.

Tzoneva, R., Seifert, B., Albrecht, W., Richau, K., Groth, T., & Lendlein, A. (2008). Hemocompatibility of poly(ether imide) membranes functionalized with carboxylic groups. *Journal of Materials Science-Materials in Medicine*, *19*(10), 3203–3210.

Vesel, A., & Mozetic, M. (2001). Behaviour of catalytic probe during surface activation of polyether sulphone. *Vacuum*, *61*(2-4), 373–377.

Vesel, A., Junkar, I., Cvelbar, U., Kovac, J., & Mozetic, M. (2008). Surface modification of polyester by oxygen- and nitrogen-plasma treatment. *Surface and Interface Analysis*, *40*(11), 1444–1453.

Wang, Y. Q., Qu, X., Lu, J., Zhu, C. F., Wan, L. J., Yang, J. L., et al. (2004). Characterization of surface property of poly(lactide-co-glycolide) after oxygen plasma treatment. *Biomaterials*, *25*(19), 4777–4783.

Washburn, E. W. (1921). The dynamics of capillary flow. *Physical Review*, *17*(3), 273–283.

Watanakunakorn, C., & Glotzbecker, C. (1978). In vitro activity of carbenicillin, ticarcillin, sisomicin and netilmicin alone and in combination against *Pseudomonas aeruginosa*. *Antimicrobial Agents and Chemotherapy*, *24*(6), 343–346.

Watthanaphanit, A., Supaphol, P., Tamura, H., Tokura, S., & Rujiravanit, R. (2010). Wet-spun alginate/chitosan whiskers nanocomposite fibers: Preparation, characterization and release characteristic of the whiskers. *Carbohydrate Polymers*, *79*(3), 738–746.

Wu, Y. B., Yu, S. H., Mi, F. L., Wu, C. W., Shyu, S. S., Peng, C. K., et al. (2004). Preparation and characterization on mechanical and antibacterial properties of chitosan/cellulose blends. *Carbohydrate Polymers*, *57*(4), 435–440.

Zemljic Fras, L., Persin, Z., & Stenius, P. (2009). Improvement of chitosan adsorption onto cellulosic fabrics by plasma treatment. *Biomacromolecules*, *10*(5), 1181–1187.